Conjugated Polyrotaxanes Incorporating Mono- or Divalent Copper Complexes

Pierre-Louis Vidal, Bernadette Divisia-Blohorn,* and Gérard Bidan*

Laboratoire d'Electrochimie Moléculaire, UMR 5819 CEA/CNRS/Université J. Fourier, Département de Recherche Fondamentale sur la Matière Condensée, CEA Grenoble, 17 rue des Martyrs, F-38054 Grenoble Cedex 9, France

Jean-Marc Kern* and Jean-Pierre Sauvage*

Laboratoire de Chimie Organo-Minérale, UMR 7513, Institut Le Bel, Université Louis Pasteur, 4 rue Blaise Pascal, F-67000 Strasbourg Cedex, France

Jean-Louis Hazemann

Laboratoire de Cristallographie, UPR 5031 CNRS, BP166, 38042 Grenoble Cedex 9, France, and Laboratoire de Géophysique Interne et Tectonophysique, UMR 5559, UJF-CNRS, BP 53, 38041 Grenoble Cedex 9, France

Received May 11, 1999

A conjugated polyrotaxane poly[Cu(**1.2**)$^{+}$] has been synthesized via copper(I)-templated strategy and electropolymerization. The polymer backbone contains alternating quaterthiophene moieties and 1,10-phenanthroline complexes. It is threaded by coordinating cyclic units. Copper(I) binding was reversible *only* if lithium cation was present during copper removal, as a labile scaffolding, maintaining the topography of the free coordinating sites and of the organic matrix, as demonstrated by ^{1}H NMR studies on monomer precursors. Electrochemistry has been coupled with X-ray absorption spectroscopy at the Cu K edge to study the interactions between the complexed copper centers and the conjugated backbone. The spectra of poly[Cu(**1.2**)$^{n+}$] in various oxidation states have been analyzed and compared with those of monomeric model compounds. For all of the samples four nitrogen atoms are the closest neighbors. No dramatic geometric and electronic differences exist between monomeric and polyrotaxane Cu(I) binding sites. However, for the copper(I) rotaxane the closest neighbors were unambiguously split into two subshells of two nitrogen atoms, reflecting higher steric constraints around the copper center in the polymetallorotaxane. For the divalent complexed copper−rotaxane, these steric constraints partially prevent the flattening of the coordination tetrahedron expected when passing from Cu(I) to Cu(II) and the Cu(II)−N distances are significantly longer in the polymer (2.04 Å) than in the model compound (2.00 Å).

Introduction

In the field of chemically modified electrodes,[1] immobilization of functionalized conducting polymers represents a very active research topic.[2] Many efforts have been devoted to the obtention of metal-containing conducting polymers, especially for their potential applications in electrocatalysis, sensor, or electronic devices.[3] Furthermore, in the past few years, various systems containing transition metal centers directly connected to the polymer backbone have been reported,[4] showing great influence of the metal on the properties of the conjugated backbone, such as photosensivity, conductivity, or fluorescence variations.

On the other hand, rotaxanes—cyclic molecules threaded by linear fragments—have been intensively studied,[5] especially in terms of photoinduced electron transfer and electro- or photochemically driven molecular motions.[6] A few years ago, we used electropolymerization of pyrrole-bearing 1,10-phenanthroline via a spacer arm to elaborate films of conducting polymetallorotaxanes[7a] using transition metals as templating agents.[8] These polymers display simultaneously the classical

(1) Abruña, H. D. *Coord. Chem. Rev.* **1988**, *86*, 135.
(2) Bidan, G. in *Polymer films in sensor applications*; Hasarsanyi, G., Ed., Technomic: Lancaster, Basel, 1995.
(3) (a) Bedioui, F.; Devynck, J.; Bied-Charreton, C. *Acc. Chem. Res.* **1995**, *28*, 30. (b) Higgins, S. J. *Chem. Soc. Rev.* **1997**, *26*, 247. (c) Swager, T. M. *Acc. Chem. Res.* **1998**, *31*, 201.
(4) (a) Yamamoto, T.; Yoneda, Y.; Maruyama, T. *J. Chem. Soc., Chem. Commun*. **1992**, 1652. (b) Wolf, M. O.; Wrighton, M. S. *Chem. Mater.* **1994**, *6*, 1526. (c) Maruyama, T.; Yamamoto, T. *Inorg. Chim. Acta* **1995**, *238*, 9. (d) Zotti, G.; Zecchin, S.; Schiavon, G.; Berlin A.; Pagani, G.; Canavesi, A. *Chem. Mater*. **1995**, *7*, 2309. (e) Zhu, S. S.; Swager, T. M. *Adv. Mater*. **1996**, *8*, 497. (f) Pickup, P. G.; Cameron, C. G. *J. Chem. Soc., Chem. Commun.* **1997**, 303. (g) Reddinger, J. L.; Reynolds, J. R. *Chem. Mater*. **1998**, *10*, 1236.
(5) (a) Sauvage, J. P. *Acc. Chem. Res.* **1990**, *23*, 321. (b) Gibson, H. W.; Bheda, M. C.; Engen, P. T. *Prog. Polym. Sci.* **1994**, *19*, 843. (c) Amabilino, D. B.; Stoddart, J. F. *Chem. Rev.* **1995**, *95*, 2725. (d) Benniston, A. C. *Chem. Soc. Rev.* **1996**, *25*, 427.
(6) (a) Collin, J. P.; Gavina, P.; Sauvage, J. P. *New J. Chem.* **1997**, *21*, 525. (b) Livoreil, A.; Sauvage, J. P.; Armaroli, N.; Balzani, V.; Flamigni, L.; Ventura, B. *J. Am. Chem. Soc.* **1997**, *119*, 12114. (c) Balzani, V.; Gomez-Lopez, M.; Stoddart, J. F. *Acc. Chem. Res.* **1998**, *31*, 405. (d) Sauvage, J.-P. *Acc. Chem. Res*. **1998**, *31*, 611.
(7) (a) Kern, J. M.; Sauvage, J. P.; Bidan, G.; Billon, M.; Divisia-Blohorn, B. *Adv. Mater.* **1996**, *8*, 580. (b) Billon, M.; Divisia-Blohorn, B.; Kern, J. M.; Sauvage, J. P. *J. Mater. Chem.* **1997**, *7*, 1169.
(8) Dietrich-Buchecker, C. O.; Sauvage, J. P. *Chem. Rev.* **1987**, *87*, 795.

10.1021/ic990516n CCC: $18.00
Published on Web 08/27/1999

properties of conducting polymers and those due to the coordinating macrocycles sliding between the nodes of the polymeric network, leading to stabilization of unusual oxidation states. We have also characterized the topological properties of such polyrotaxanes. [7b]

More recently, we and others published related works with U-shaped 1,10-phenanthroline[9] or linear 2,2′-bipyridine[10] directly connected to electropolymerizable thienyl derivatives, in an effort to better control the structure and to improve electronic coupling between the rotaxane coordinating site and the conjugated backbone.

In a previous communication,[9] we described a coordinating polyrotaxane poly[Cu(**1.2**)$^+$] with a conjugated backbone alternating quaterthiophene moieties and 1,10-phenanthroline complexes with threaded cyclic units. We now report the synthesis of the precursors and of the electropolymerized material as well as the results of a study combining electrochemistry and X-ray absorption spectroscopy. In particular, it was possible from in situ XANES and EXAFS studies to estimate the oxidation state of the metal and its chemical surroundings under various electrochemical conditions.

Results and Discussion

Precursors. The strategy used to prepare the threaded copper(I) complex Cu(**1.2**)BF_4, the precursor of the polymetallorotaxanes studied in this work, is reminiscent of that which allowed the first synthesis of a tetrahedral copper(I) catenate on a preparative scale by some of us.[11] It relies on the three-dimensionnal assembling and templating effect of copper(I), which forces the acyclic fragment **1** to thread through ring **2**, the driving force for such a process being the formation of a very stable bis(2,9-diaryl-1,10-phenanthroline)copper(I) complex[12] (Scheme 1). Thus Cu(**1.2**)$^+$ was prepared in two steps, the first one consisting of the formation of Cu(**2**)$^+$ where the metal is only complexed by one chelate, i.e., the coordinating moiety of the macrocycle **2**. In a second step, threading of the molecular string **1** through Cu(**2**)$^+$ leads to the polymetallorotaxane precursor Cu(**1.2**)$^+$, where the electropolymerizable subunit **1** is threaded through the coordinating macrocycle **2**.

The synthesis of the dpp-containing macrocycle **2** (dpp = 2,9-diphenyl-1,10-phenanthroline) has already been extensively described.[13] The design of **1** is based on a previous observation[14] which showed that disubstitution of 1,10-phenanthroline by a *single* thiophene unit followed by complexation with copper(I) leads by electropolymerization to the deposition of a monolayer which does not contain copper, presumably due to steric hindrance around the metal after polymerization and/or to the too high electrodeposition potential required. CPK molecular models suggested that lengthening of the oligothiophene spacer could increase the flexibility of the polymer thread. On the other hand, extension of the electroactive oligothienyl units should lower their oxidation potential. **1**, where the 2,9-positions of the phenanthroline are substituted by bithienyl units, was then chosen as the key electropolymerizable ligand. It was prepared in two steps, by successive additions of 5-lithio-2,2′-bithiophene (overall yield: 18%) (Figure 1). Each addition is followed by hydrolysis of the resulting adduct and rearomatization with a strong oxidative agent.

Scheme 1. Synthesis of the Threaded Complex Cu(**1.2**)$^+$ and of the Polyrotaxane Poly(Cu(**1.2**)$^{2+}$)

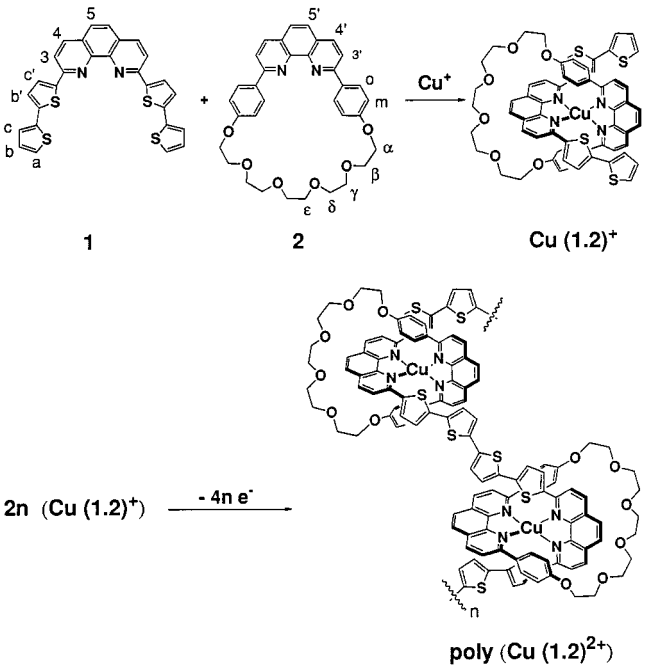

The relatively poor yield of the second addition step of 5-lithio-2,2′-bithiophene can be attributed to the deactivation of the monoadduct toward nucleophilic addition due to the electron-donating effect of the bithienyl substituent already present. **1** is isolated as an air- and light-stable yellow-brown solid and exhibits fairly good solubility in CH_3CN or CH_2Cl_2.

Reaction between **2** and a slight deficit of $Cu(CH_3CN)_4BF_4$ followed by the addition of **1** in a CH_3CN/CH_2Cl_2 mixture led to the threaded heteroleptic complex Cu(**1.2**)BF_4, isolated after chromatography in 95% yield as a dark red powder. This intense red color is typical of a metal-to-ligand charge transfer (MLCT)[15] process. Cu(**1.2**)BF_4 is an air- and light-stable complex which exhibits good solubility in CH_3CN or CH_2Cl_2.

Electrooxidative Deposition of the Polymer. The polymetallorotaxane polyCu(**1.2**)$^+$ was prepared by oxidative electropolymerization of the threaded precursor Cu(**1.2**)$^+$. A platinum disk electrode was dipped into a dilute solution of Cu(**1.2**)$^+$ in dichloromethane containing tetrabutylammonium hexafluorophosphate as the supporting electrolyte. Continuous cycling of the potential of this electrode between −0.2 and 1.4 V led to the deposition of a film onto the electrode surface. This film being electroactive, its deposition could be monitored by recording of the current/potential curves along the potential cycling process.

The modified electrode so obtained was washed and dried, and after dipping in a fresh electrolyte solution, the electrochemical behavior of the deposited matter was determined by cyclic voltammetry[9] (Figure 2a). The redox system at 0.51 V is characteristic of the $Cu(dpp)_2$[16] moiety. At 50 mV s^{-1} a partial

(9) Vidal, P. L.; Billon, M.; Divisia-Blohorn, B.; Bidan, G.; Kern, J. M.; Sauvage, J. P. *J. Chem. Soc., Chem. Commun.* **1998**, 629.
(10) Zhu, S. S.; Swager, T. M. *J. Am. Chem. Soc.* **1997**, *119*, 12568.
(11) (a) Dietrich-Buchecker, C. O.; Sauvage, J. P.; Kintzinger, J. P. *Tetrahedron Lett.* **1983**, *24*, 5095. (b) Dietrich-Buchecker, C. O.; Sauvage, J. P.; Kern, J. M. *J. Am. Chem. Soc.* **1984**, *106*, 3043.
(12) (a) Chambron, J.-C.; Dietrich-Buchecker, C. O.; Nierengarten, J.-F.; Sauvage, J.-P. *New J. Chem.* **1993**, *17*, 331. (b) Chambron, J.-C.; Dietrich-Buchecker, C.; Nierengarten, J.-F.; Sauvage, J.-P.; Solladie, N.; Albrecht-Gary, A.-M.; Meyer, M. *New J. Chem.* **1995**, *19*, 409.
(13) Dietrich-Buchecker, C. O.; Sauvage, J.-P. *Tetrahedron* **1990**, *46*, 503.
(14) Bidan, G.; Billon, M.; Divisia-Blohorn, B.; Leroy, B.; Vidal, P. L.; Kern, J. M.; Sauvage, J. P. *J. Chim. Phys.* **1998**, *95*, 1254.
(15) Gushurst, A. K. I.; McMillin, D. R.; Dietrich-Buchecker, C. O.; Sauvage, J. P. *Inorg. Chem.* **1989**, *28*, 4070.
(16) Dietrich-Buchecker, C. O.; Sauvage, J. P.; Kern, J. M. *J. Am. Chem. Soc.* **1989**, *111*, 7791.

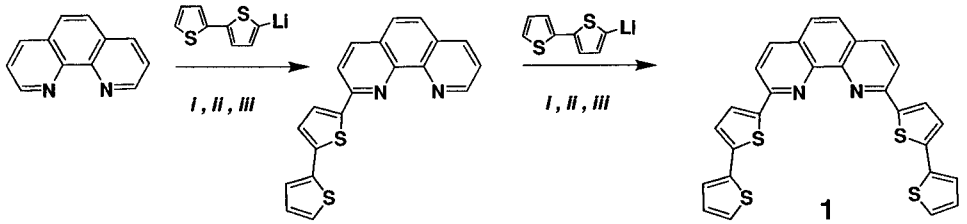

Figure 1. Synthesis of the electropolymerizable ligand **1**: (i) addition of 1.5 equiv of 5-lithio-2,2′-bithiophene in THF/toluene; (ii) H_2O; (iii) MnO_2.

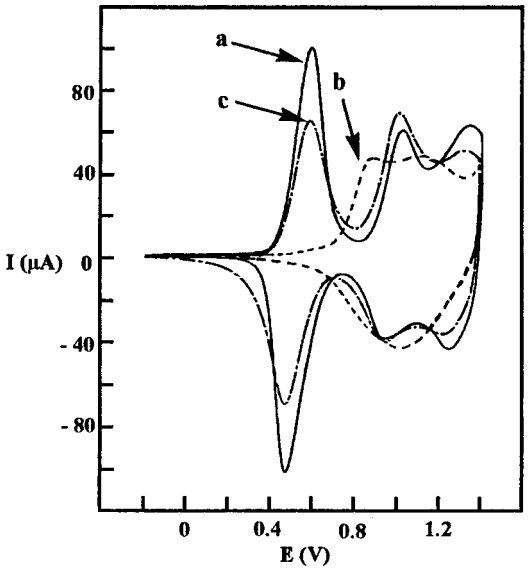

Figure 2. Cyclic voltammetry in CH_2Cl_2 + 0.3 mol L^{-1} Bu_4NPF_6 (v = 50 mv/s) of a poly[Cu(**1**.**2**)$^+$] film (a) freshly prepared (solid line), (b) after dipping (20 min) in a 0.1 mol L^{-1} $LiClO_4$ + 0.1 mol L^{-1} Bu_4NCN/CH_3CN solution (dashed line), and (c) after dipping (3 h) in a 0.1 mol L^{-1} $Cu(CH_3CN)_4BF_4/CH_3CN$ solution (dot−dashed line).

loss of reversibility was observed by comparison with the behavior of the free monomer, but at a slower potential sweep rate (10 mV s^{-1}), the ΔE_p value observed (20 mV) is typical of immobilized electroactive systems. The response between 0.8 and 1.4 V consists of two well-defined waves, in agreement with the electrochemical behavior of end-capped tetrathienylenes,[17] and confirms the electrocoupling of the terminal bithienyl units. The same procedure was followed to deposit polymetallorotaxanes onto gold or carbon felt electrodes.

Demetalation−Remetalation Behavior. In the course of demetalation−remetalation experiments aimed at testing the ability of the polymer film prepared above to be used as a sensor for various metal ions, we discovered an original structural effect: The copper(I) template used to assemble the fragments of the precursor could be removed by dipping the material into a cyanide solution, taking into account the high affinity of Cu(I) for cyanide ions. Interestingly, subsequent remetalation was only possible if Li^+ was present during the copper removal. This scaffolding effect is depicted in Scheme 2 and corresponding cyclic voltammetries are in Figure 2.

A strong cathodic shift (140 mV) of the electrochemical response of the oligothienyl wire was observed when copper was removed. This effect can be explained by considering the electron-withdrawing effect of the copper(II)−phenanthroline complex fragments onto the conjugated backbone, making the oligothienyl moiety more difficult to oxidize in the metal-containing material than in the metal-free state.

(17) (a) Baüerle, P. *Adv. Mater*. **1992**, *4*, 102. (b) Zotti, G.; Schiavon, G.; Berlin, A.; Pagani, G. *Chem. Mater*. **1993**, *5*, 430.

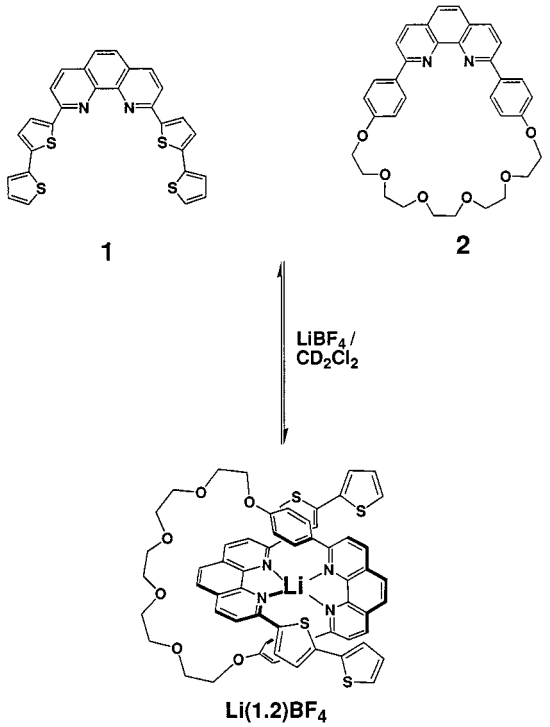

Figure 3. Lithium binding mode in the precursor.

The function of lithium is assumed to be that of an ionic scaffold, maintaining the topography of the coordination sites after copper removal. This behavior can be explained both by the poor affinity of lithium for cyanide and by its known ability to form *labile* complexes with dpp ligands.[16] However, nitrogen, oxygen, and sulfur are all donor atoms, and a variety of binding modes for lithium cations can exist in the polymeric network. The highly reducing potential required for an electrochemical study of lithium complexes[16] is not compatible with the limited cathodic range of CH_2Cl_2. However, cycling our structure in the cathodic range (0 to −2 V vs Ag^+/Ag reference) in 0.1 mol L^{-1} Bu_4NPF_6/CH_3CN results in a rapid loss of the electroactivity after a few cycles. We thus decided to investigate lithium complexation by ^1H NMR spectroscopy on the monomer precursors so as to evidence formation of bis(dpp)-type Li^+ complexes. $LiBF_4$ was added to a pale yellow mixture of **1** and **2** in CD_2Cl_2 (1:1:1 stoichiometry). Subsequently ^1H NMR and COSY spectra of this mixture were recorded. Formation of Li(**1**.**2**)$^+$ (see Figure 3) with the well-known bis(dpp)-type entwined topography was then spectroscopically evidenced, besides other compounds.

As shown in Table 1, H_m and H_o signals for this compound exhibit the same strong upfield shifts observed for Cu(**1**.**2**)BF_4 as compared to free macrocycle **2**. $H_{b'}$ and $H_{c'}$ exhibit upfield shifts upon complexation by lithium similar to those observed upon complexation by copper template. However, signals from the free ligands were still present, as a result of the poor stability

Scheme 2. Scaffolding Effect

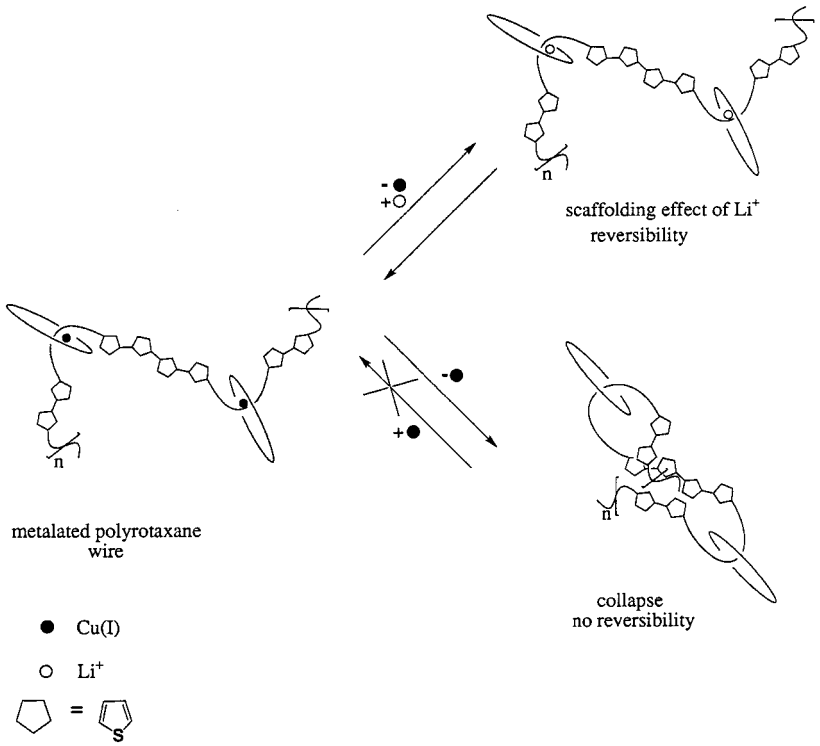

Table 1. Selected ^{1}H NMR Chemical Shifts (in ppm) (400 MHz, CD_2Cl_2) for Free Ligands and Prerotaxane Complexes

signals	**1**	**2**	Cu(**1.2**)$^+$	Li(**1.2**)$^+$
H_o		8.42	7.32	7.30
H_m		7.23	5.96	6.05
$H_{c'}$	7.74		7.24	7.10
$H_{b'}$	7.27		6.65	6.54

of this lithium complex, and attempts to isolate Li(**1.2**)BF_4 were unsuccessful.

Accordingly, we attribute this ionic scaffolding effect of lithium to the formation of a bis(dpp) lithium complex—the nitrogen atoms of the phenanthroline being the coordinating atoms—which maintains the topography of the coordination site and whose relative lability allows easy remetalation with Cu(I) species.

XAS Spectroscopy. In order to gain more information about the interactions between copper and the conjugated structure, we have coupled electrochemistry with X-ray absorption (XAS) spectroscopy.[18] XAS spectroscopy represents indeed a highly sensitive tool to study atomic and molecular structures of noncrystalline materials such as electrochemical interfaces,[19] but surprisingly, to our knowledge only few EXAFS or XANES studies have been published on conducting polymers.[19,20] So we have undertaken an X-ray absorption study on poly[Cu(**1.2**)$^+$] at the Cu K edge at different potentials, and we now describe the in situ XANES and EXAFS experiments which have allowed us to determine the oxidation state of the copper ion (I or II) and moreover to investigate quantitatively the transformation of its local environment (number of neighboring atoms, distribution and values of bond lengths) in the polyrotaxane, by comparison with monomeric model complexes.

Two reference compounds (Figure 4), $Cu^I(dap)_2BF_4$ and $Cu^{II}(dap)_2(BF_4)_2$[16] [dap = 2,9-di(*p*-anisyl)-1,10-phenanthroline], have been selected for their chemical environment as close as possible to the one envisaged for the present polymer.

Furthermore, crystal structures of these compounds[21] or related dpp complexes[22] have previously been reported: the coordination geometry for the copper (I) center in $[Cu(dap)_2]^+$ (Cu−N bond distances: 2.053 and 2.067 Å) or $[Cu(dpp)_2]^+$ (Cu−N bond distances: 2.019 and 2.112 Å for one dpp, 2.032 and 2.082 Å for the other) is best described as distorted and dissymmetrical tetrahedral. The coordination geometry for the copper(II) center in $[Cu(dpp)_2]^{2+}$ (Cu−N bond distances between 1.98 and 1.997 Å) is best described as flattened tetrahedral, with no additional ligand, which is quite unusual for copper(II) bis(diimine) complexes.[22]

We have recorded the XAS spectra of $Cu^I(dap)_2BF_4$ and $Cu^{II}(dap)_2(BF_4)_2$ reference solutions and then the spectra of poly[Cu(**1.2**)$^{n+}$] in supporting electrolyte polarized successively at E = 0 V (spectrum of poly[Cu(**1.2**)$^+$]) and E = 0.9 V (spectrum of poly[Cu(**1.2**)$^{2+}$]). The choice of this last potential value was dictated by the generation of the +II redox state for copper combined with the conservation of the conjugated structure, sensitive to long-time polarization in the oxidized state (the average acquisition time for one EXAFS spectrum is approximately 1 h). At the end of the acquisition, a spectrum of the polymer polarized again at 0 V was recorded in order to check the stability of the structure to the polarization and to

(18) For a theoretical description of EXAFS spectroscopy: Stern, E. A. In *X-ray Absorption Principles, Applications, Techniques of EXAFS, SEXAFS and XANES*; Koninsberger, D. C., Prins, R., Eds.; Wiley-Interscience: New York, 1988.

(19) Abruña, H. D.; White, J. H.; Albarelli, M. J.; Bommarito, G. M.; Bedzyk, M. J.; McMillan, M. *J. Phys. Chem.* **1988**, *92*, 7045.

(20) (a) Tourillon, G.; Dexpert, H.; Lagarde, P. *J. Electrochem. Soc.* **1987**, *134*, 327. (b) Tourillon, G.; Flank, A. M.; Lagarde, P. *J. Phys. Chem.* **1988**, *92*, 4397. (c) Igo, D. H.; Elder, R. C.; Heineman, W. R. *J. Electroanal. Chem.* **1991**, *314*, 45. (d) Billon, M.; Bidan, G.; Divisia-Blohorn, B.; Kern, J. M.; Sauvage, J. P.; Parent, P. *J. Electroanal. Chem.* **1998**, *456*, 91.

(21) Geoffroy, M.; Wermeille, M.; Buchecker, C. O.; Sauvage, J. P.; Bernardinelli, G. *Inorg. Chim. Acta* **1990**, *167*, 157.

(22) Miller, M. T.; Gantzel, P. K.; Karpishin, T. B. *Inorg. Chem.* **1998**, *37*, 2285.

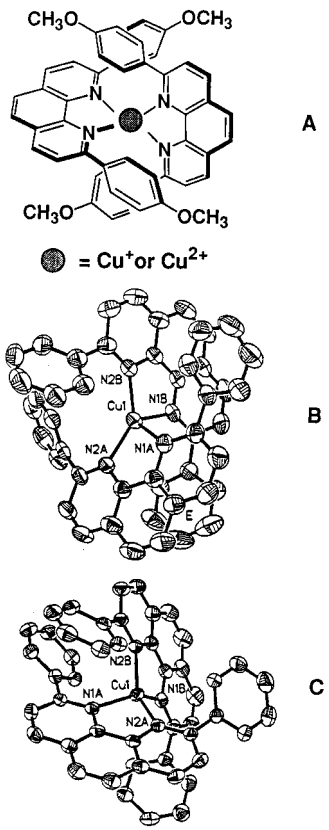

Figure 4. (A) Cu(I) or Cu(II) bis[2,9-di(*p*-anisyl)-1,10-phenanthroline]. (B and C) X-ray structures of respectively Cu(I) and Cu(II) bis [2,9-diphenyl-1,10-phenanthroline], adapted from ref 22.

the X-ray exposure. However, no difference between this spectrum and the initial spectrum recorded at $E = 0$ V was observed.

XANES Study. The shapes of the XANES spectra are very sensitive to the electronic structure and to the geometry around the copper ion.[23,24] Actually, this region corresponds to forbidden 1s → 3d and allowed 1s → 4p transitions of the excited photoelectron to vacant bound states of p-symmetry, and the ordering of those vacant orbitals is dependent on the geometry of the copper coordination sphere. Therefore, a qualitative comparative XANES study between reference compounds and polymeric samples has been undertaken before EXAFS analysis to gain structural information from polymetallorotaxane poly-[Cu(**1.2**)$^{n+}$]) as a function of the potential applied. The spectra are shown in Figure 5.

First of all, the intensity of the so-called white line in the 8994−8996 eV region is nearly the same for all of the samples. The XANES spectra of the reference copper complexes $Cu^{I}(dap)_2BF_4$ and $Cu^{II}(dap)_2(BF_4)_2$ exhibit typical behavior of copper in respectively I and II oxidation states: for $Cu^{I}(dap)_2$-BF_4 the spectrum displays a first strong transition (prepeak transition) at 8985 eV, then the white line at 8995 eV and a shoulder at 9005 eV. These two successive transitions result from the well-known distortion[22] of the tetrahedral environment for this Cu(I) complex: this leads to a split of the 4p orbitals.[23] Therefore the two successive transitions have been assigned respectively to 1s → $4p_z$ and 1s → $4p_{xy}$ ones.[20d] The XANES of $Cu^{II}(dap)_2(BF_4)_2$ displays a shift of the edge energy of +2 eV compared to the Cu(I) reference. A weak peak is present at

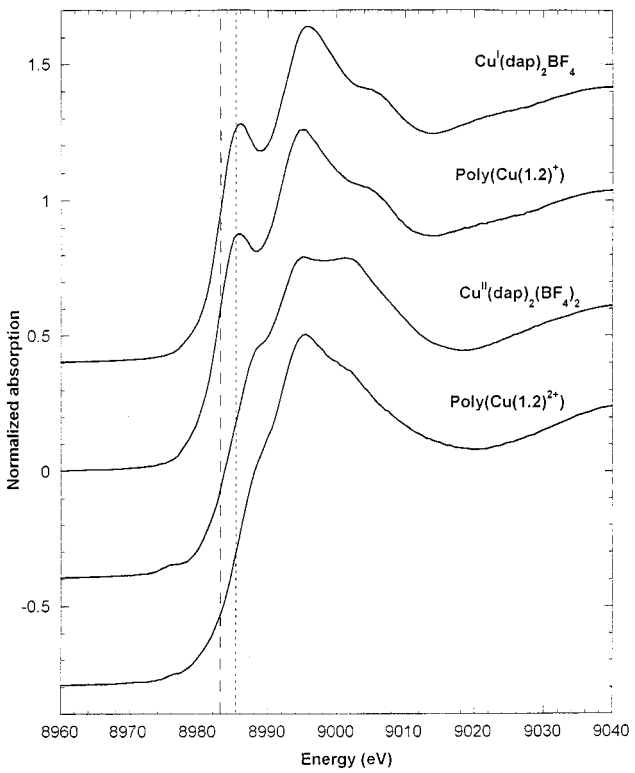

Figure 5. XANES spectra of the monomer compounds and of the polymetallorotaxane samples.

8976 eV, which corresponds to the 1s → 3d transition (this transition is absent in the Cu(I), d^{10} compound) and then a shoulder at 8988 eV followed by two main peaks at 8995 and 9002 eV.

For the polymer samples, poly[Cu(**1.2**)$^{+}$] displays the same shape as $Cu^{I}(dap)_2BF_4$ without any edge energy shift: this suggests that the electronic structure and the topography of the Cu(I) binding sites are very similar in both cases. The shape of the poly[Cu(**1.2**)$^{2+}$] sample shows an edge energy shift similar to that for $Cu^{II}(dap)_2(BF_4)_2$ but displays several differences with respect to this spectrum: the prepeak corresponding to the 1s → 3d transition is weaker, whereas the shoulder at 8988 eV has disappeared and the intensity of the second main peak at 9002 eV has dramatically decreased. Therefore the geometry around Cu(II) centers seems to be strongly modified when passing from a monomeric Cu(II) compound to a polarized polymetallorotaxane.

EXAFS Study. The structural parameters deduced from analysis of the spectra are summarized in Table 2 whereas Fourier-filtered first shell and corresponding best fits are presented in Figure 5. In all of the cases, EXAFS identifies four nitrogen atoms as the closest neighbors. It is worth noting that all attempts to include one additional boron, nitrogen, or phosphorus atom (especially for Cu(II) compounds) by the way of a second shell do not improve the fit or lead to a worse one. When necessary, splitting of those neighbors into subshells has been simulated: all combinations $N_xN_yN_zN_w$ ($x + y + z + w = 4$) have been considered.

For $[Cu(dap)_2]^{2+}$, the best fit with McKale functions[25] was obtained with four nitrogen nearest neighbors at a distance of 2.00 Å with a σ^2 value indicative of a quite narrow distance distribution, in total accordance with the coordination geometry recently described for the related dpp complex.[22] Then the data

(23) Kau, L. S.; Spira-Solomon, D. J.; Penner-Hahn, J. E.; Hodgson, K. O., Solomon, E. I. *J. Am. Chem. Soc.* **1987**, *109*, 6433.
(24) Sano, M.; Komorita, S.; Yamatera, H. *Inorg. Chem.* **1992**, *31*, 459.
(25) McKale, A. G.; Knapp, G. S.; Chan, S. K. *J. Am. Chem. Soc.* **1988**, *110*, 3763.

Table 2. Cu−N Distances for the Fits of the Different Samples (Values in Parentheses Are Estimated Uncertainties in the Last Digit)

sample	R_1 (Å)	$\sigma_1^2 \times 10^3$ (Å^2)	R_2 (Å)	$\sigma_2^2 \times 10^3$ (Å^2)
$[Cu(dap)_2]^{+}$ [a]				
4N	2.03 (0.7)	7.1 (5)		
2N2N	1.98 (0.4)	4.6 (5)	2.08 (0.4)	4.3 (5)
$[Cu(dap)_2]^{2+}$ [b]				
4N	2.00 (1)	4.6 (7)		
poly[Cu(**1.2**)$^{+}$] [a]				
4N	2.03 (0.5)	8.1 (7)		
2N2N	1.97 (0.6)	1.6 (7)	2.11 (0.6)	1.4 (7)
poly[Cu(**1.2**)$^{2+}$] [b]				
4N	2.04 (0.5)	7.1 (6)		

[a] $\Delta E_0 = -1.9$. [b] $\Delta E_0 = 0$.

for $Cu(dap)_2]^{+}$ were fitted either with McKale functions or with phase and amplitude functions extracted from $[Cu(dap)_2]^{2+}$. The results of these two fits are identical, and the optimized average bond length is 2.03 Å, with a significantly broader distribution distance than for the monomeric Cu(II) compound. Attempts to split the neighbors into two subshells of two nitrogen atoms do not improve the fit, and the σ^2 values obtained are only slightly lowered (Table 2). Assessing the distances to the longer reported values[21,22] (2.05−2.06 Å) results in a worsening of the fit in terms of phase. We then chose the phase and amplitude functions extracted from $[Cu(dap)_2]^{2+}$ to fit the polymetallorotaxane samples, because of its best fit adequacy with crystallographic data. Furthermore, we found that the narrowness of its distance distribution would be particularly useful to split the different nitrogen neighbors' shell in the polymer.

Observation of the poly[Cu(**1.2**)$^{+}$] EXAFS spectrum reveals the presence of an important beating for $k = 11$ Å^{-1} which may correspond to two out of phase subshells (Figure 6). The oscillations for the high k values could indeed never be described by a single shell of four nitrogen atoms (4N modelization), and the best fit has been obtained upon splitting these closest neighbors into two subshells of two nitrogens each (2N2N modelization), with quite remote distances of 1.97 and 2.11 Å and with a very narrow distribution. This beating disappeared in poly[Cu(**1.2**)$^{2+}$] spectra (Figure 6). The fit for a 4N environment for the Fourier-filtered first shell of poly[Cu(**1.2**)$^{2+}$] could not completely describe the oscillations at high k values in terms of phase. The 2N2N modelization gave quite similar results, but the higher Cu(II)−N distance obtained with this modelization (2.11 Å) is not acceptable. Attempts to improve the fit by adding a neighbor or trying other splitting combinations were unsuccessful. Surprisingly, going from poly[Cu(**1.2**)$^{+}$] to poly[Cu(**1.2**)$^{2+}$], the average distance of nitrogen atoms to the copper center becomes slightly longer (Table 2), but these differences are small and within the usual uncertainty of EXAFS-determined bond distances.

The similarity of XANES, distances, and corresponding Debye−Waller factors obtained with a 4N model (Table 2) for poly[Cu(**1.2**)$^{+}$] and $[Cu(dap)_2]^{+}$ reveals that there are no fundamental geometric or electronic differences between monomeric and analogous polyrotaxane Cu(I) binding sites. However, poly[Cu(**1.2**)$^{+}$] is unambiguously best modeled by a 2N2N simulation (Figure 6), as further confirmed by the significant lowering of corresponding Debye−Waller factors in this case.

The longer distance obtained (2.11 Å) is in the range of crystallographic data previously reported,[22] whereas the shorter one (1.97 Å) is unusually low for a Cu(I)−N bond. On the contrary, for the $[Cu(dap)_2]^{+}$ spectrum, the splitting into two subshells is not evident, and the distances obtained with a 2N2N

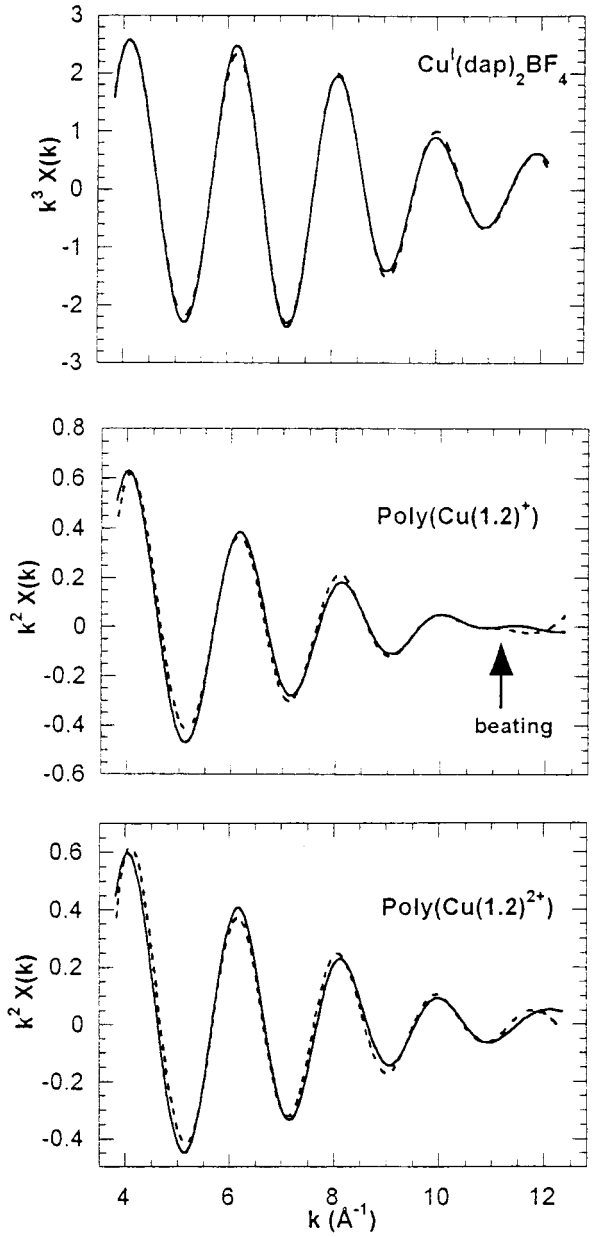

Figure 6. Fourier-filtered first shell of the different samples (solid line) and corresponding best fits (dashed line) for a 4N environment $[Cu(dap)_2]^{+}$, poly[Cu(**1.2**)$^{2+}$]) or a 2N2N environment (poly[Cu(**1.2**)$^{+}$]).

modelization are less spread apart than with poly[Cu(**1.2**)$^{+}$] (Table 2). This difference certainly reflects slightly higher steric constraints around the copper(I) center in the polymetallorotaxane than in the monomeric model compound.

On the other hand, the shapes of XANES are unambiguously different for poly[Cu(**1.2**)$^{2+}$] and $[Cu(dap)_2]^{2+}$, indicating strong differences for Cu(II) binding site topography. The disappearance of the beating at high k values for poly[Cu(**1.2**)$^{2+}$] reveals important changes in the distance distribution compared to poly[Cu(**1.2**)$^{+}$]. However, analysis of the Debye−Waller factors reveals only a very slight narrowing of the average distance distribution to the nitrogen nearest scatterers in poly[Cu(**1.2**)$^{2+}$] compared to poly[Cu(**1.2**)$^{+}$] (Table 2), contrary to what is observed when passing from $[Cu(dap)_2]^{+}$ to $[Cu(dap)_2]^{2+}$ monomer analogues. This suggests that strong steric constraints inside the polymer partially prevent flattening of the coordination tetrahedron, as usually observed when passing from Cu(I) to Cu(II) in monomeric analogues.[21,22] Furthermore, there is no

lowering of the Cu−N distance upon polarization, contrary to what is expected when going from the Cu(I) to the Cu(II) state, and the Cu(II)−N distances are significantly longer in the polymer (2.04 Å) than in the monomeric compound (2.00 Å).

Further studies are currently in progress on conductivity measurements coupled with electrochemistry by means of microelectrode devices to show the respective impacts of copper and lithium coordination on the electronic properties of the conjugated polyrotaxane.

Conclusion

In conclusion, a new type of conjugated polyrotaxane has been made, the construction principle being based on the gathering and threading effect of monovalent copper, which forces a bithienyl-disubstituted chelate to thread through a coordinating ring. Subsequent electropolymerization of the monomeric precursor afforded a conductive film which could be demetalated. Unexpectedly, the film could not be recomplexed with copper(I) unless Li^+ was present during the demetalation, leading to a new property. This effect can be viewed as a scaffolding effect. The lithium cation occupies in a loose manner the coordination sites in a transitory fashion, thus preventing the organic backbone and the complexation sites from collapsing. A detailed XAS study has been carried out which brings firm evidence that the copper metal environment in the film is not substantially different from that in the precursors or model compounds, regardless of the oxidation state. An interesting observation is that, in the polymer film, the matrix imposes severe steric constraint which seems to lower the symmetry of the copper(I) complex, the four nitrogen atoms which constitute the coordination sphere now becoming different two by two. The strong cathodic shift of the doping potential of the Li^+-complexed rotaxane compared to that of the copper−polyrotaxane gives evidence of the coupling of the metal center and the quaterthienyl wire.

Experimental Section

Reagents and Chemical and Electrochemical Procedures. Air- and moisture-sensitive reactions were carried out in oven-dried glassware under an argon atmosphere. CH_3CN and toluene were distilled from CaH_2. THF was distilled from sodium benzophenone immediatly before use. CH_2Cl_2 used for electrochemical experiments was distilled from P_2O_5 and stored in a drybox under an argon atmosphere. Cu-$(CH_3CN)_4BF_4$ was prepared as previously described.[16] *n*-Bu_4NPF_6 was dried at 100 °C under vacuum and stored in a desiccator, and all other commercially available reagents were used as received. ^{1}H NMR spectra were recorded with a AC-200 Bruker or a U-400 Varian spectrometer. Mass spectral analyses were performed by the Institut de Biologie Structurale, Grenoble, France. Electrochemical synthesis and studies were performed in a drybox under an argon atmosphere (except polarization of films for EXAFS spectroscopy measurements) using a PAR 273A from EG&G Princeton Applied Research and with a typical three-electrode cell. The electrolyte solutions used were all 0.3 mol L^{-1} *n*-Bu_4NPF_6 in CH_2Cl_2. A 0.07 cm^2 platinum or gold electrode was used as the working electrode. Potentials were relative to a 0.01 mol L^{-1} Ag^+/Ag reference electrode ($E_{1/2}$ (ferrocene) = 0.18 V and $E_{1/2}$ (Cu(dap)$_2$BF$_4$) = 0.48 V vs this reference for 10^{-3} mol L^{-1} solutions in the same supporting electrolyte). Electrosynthesis of the polyrotaxane films was performed from 2×10^{-3} mol L^{-1} monomer solutions by continuous cycling between −0.2 and 1.4 V at υ = 50 mV/s. The films obtained were then copiously washed with fresh CH_2Cl_2 before cycling. For demetalation experiments, cyanide solution was made from *n*-Bu_4NCN dissolved in CH_3CN and lithium/cyanide solution from stoichiometric amounts of *n*-Bu_4NCN and $LiClO_4$ dissolved in CH_3CN. The films were dipped for 20 min in one of these solutions and washed with CH_3CN and then with CH_2Cl_2 before cycling. Remetalations were performed by dipping films for 1 h in a copper(I) solution made from Cu$(CH_3CN)_4BF_4$ dissolved in CH_3CN, followed by copious rinsing with fresh CH_3CN and then CH_2Cl_2.

2-(2,2′-Bithien-5-yl)-1,10-phenanthroline. A solution of diisopropylamine (4.25 mL, 30 mmol) in 50 mL of THF was cooled to −78 °C. To this solution was then added dropwise *n*-butyllithium (18.75 mL, 1.6 mol L^{-1} in hexane, 30 mmol). The mixture was stirred at −78 °C for 15 min, allowed to warm to 5 °C for 20 min, and then recooled to −78 °C. A solution of 2,2′-bithiophene (5 g, 30 mmol) dissolved in 100 mL of THF was then added via the double-ended needle technique. This mixture was stirred at −78 °C for 30 min, allowed to rise to 0 °C, and then added to a colorless solution of 1,10-phenanthroline (3.6 g, 20 mmol) in 100 mL of THF/toluene (1:1) at room temperature. A red dark color appeared immediately, and after this mixture was stirred at room temperature for 16 h, saturated water with NH_4Cl was slowly added. After removal of organic solvents, CH_2Cl_2 (150 mL) was added and the organic layer was separated. Fifty grams of MnO_2 was progressively added to this vigorously stirred dark brown solution within 1 h, until complete rearomatization had occurred (the reaction was monitored by thin layer chromatography). Addition of magnesium sulfate (50 g) and additionnal stirring for 15 min was followed by filtration on Celite and evaporation of the filtrate. This residue was chromatographed (silica gel, progressive elution from CH_2Cl_2 to 2% MeOH/CH_2Cl_2) to give 3.45 g of pure 2-(2,2′-bithien-5-yl)-1,10-phenanthroline (50%) as a dark brown solid poorly soluble in common organic solvents. ^{1}H NMR (200 MHz, $CDCl_3$): δ (ppm) 9.25 (dd, 1H), 8.24 (dd, 1H), 8.22 (d, 1H), 7.99 (d, 1H), 7.77−7.73 (m, 3H), 7.63 (dd, 1H), 7.35 (dd, 1H), 7.28−7.24 (m), 7.07 (dd, 1H). FABMS: *m*/*z* 345.0 [MH^+], 179.1, 166.

2,9-Bis(2,2′-bithien-5-yl)-1,10-phenanthroline (1). In a similar procedure, 5-lithio-2,2′-bithiophene (7.3 mmol) in 40 mL of THF at 0 °C was added to an orange brown solution of 2-(2,2′-bithien-5-yl)-1,10-phenanthroline (2.29 g, 6.65 mmol) in 150 mL of THF. The solution turned red dark immediately and was stirred for 16 h at room temperature. Hydrolysis, extraction with CH_2Cl_2, rearomatization by MnO_2 (25 g), and then chromatography (silica gel, CH_2Cl_2) led to the desired compound (490 mg), isolated as an air- and light-stable yellow-brown solid (36% yield, for a conversion rate of 40%). ^{1}H NMR (400 MHz, CD_2Cl_2): δ (ppm) 8.20 (H_4, d, ^3J (H_4,H_3) = 8.3 Hz, 2H), 7.95 (H_3, d, ^3J (H_3,H_4) = 8.3 Hz, 2H), 7.74 ($H_{c'}$, d, ^3J ($H_{c'}$,$H_{b'}$) = 3.8 Hz, 2H), 7.70 (H_5, s, 2H), 7.42 (H_a, dd, ^3J (H_a,H_b) = 3.5 Hz, ^4J (H_a,H_c) = 1.1 Hz, 2H), 7.29 (H_c, dd, ^3J (H_c,H_b) = 5.1 Hz, ^4J (H_c,H_a) = 1.1 Hz, 2H), 7.27 ($H_{b'}$, d, ^3J ($H_{b'}$,$H_{c'}$) = 3.8 Hz, 2H), 7.09 (H_b, dd, ^3J (H_b,H_a = 3.5 Hz, ^3J (H_b,H_c) = 5.1 Hz, 2H). FABMS: *m*/*z* 509.0 [MH^+], 345. Anal. Calcd for $C_{28}H_{16}N_2S_4$: C, 66.11; H, 3.17; N, 5.51. Found: C, 66.31; H, 3.09; N, 5.29.

Cu(1.2)BF$_4$. By the double-ended needle transfer technique, Cu-$(CH_3CN)_4BF_4$ (13 mg, 41 mmol) dissolved in 5 mL of CH_3CN was added to a yellow pale solution of **2** (23 mg, 40 mmol) in 5 mL of CH_2Cl_2. A deep orange coloration appeared immediately. After 30 min at room temperature, **1** (19 mg, 37 mmol) dissolved in 5 mL of CH_2Cl_2 was added, and the solution turned red brown immediately and was stirred for 40 min. The solvents were removed under vacuum, and the product was redissolved in CH_2Cl_2 and then washed with H_2O containing a small amount of ascorbic acid. Filtration (silica gel, 5% MeOH/ CH_2Cl_2) gave the desired product (43 mg, 95%) as a red dark powder. ^{1}H NMR (CD_2Cl_2, 400 MHz): δ (ppm) 8.54 (H_4, d, ^3J (H_3,H_4) = 8.5 Hz, 2H), 8.42 ($H_{4'}$, d, ^3J ($H_{4'}$,$H_{3'}$) = 8.3 Hz, 2H), 8.17 (H_5, s, 2H), 7.91 ($H_{5'}$, s, 2H), 7.89 (H_3, d, ^3J (H_3,H_4) = 8.5 Hz, 2H), 7.86 ($H_{3'}$, d, ^3J ($H_{3'}$,$H_{4'}$) = 8.3 Hz, 2H), 7.32 (H_o, d, ^3J (H_o,H_m) = 8.8 Hz, 4H), 7.24 ($H_{c'}$, d, ^3J ($H_{c'}$,$H_{b'}$) = 3.9 Hz, 2H), 7.10 (H_a, dd, ^3J (H_a,H_b) = 5.1 Hz, ^4J (H_a,H_c) = 1.2 Hz, 2H), 6.78 (H_b, dd, ^3J (H_b,H_a) = 5.1 Hz, ^3J (H_b,H_c) = 3.8 Hz, 2H), 6.65 ($H_{b'}$, d, ^3J ($H_{b'}$,$H_{c'}$) = 3.9 Hz, 2H), 6.17 (H_c, dd, ^3J (H_c,H_b) 3.8 Hz, ^4J (H_c,H_a) = 1.2 Hz, 2H), 5.96 (H_m, d, ^3J (H_m,H_o) = 8.8 Hz, 4H), 3.85−3.40 (H_α, H_β, H_γ, H_δ, H_ϵ, m, 20H). FABMS (*m*/*z*): 1137.2 ([M − BF_4]$^+$), 629.2 ([M − 1 − BF_4]$^+$), 570.9 ([M − 2 − BF_4]$^+$), 509.0 ([1H]$^+$). Anal. Calcd for C_{62} $H_{50}N_4O_6S_4$-CuF_4: C, 60.76; H, 4.11; N, 4.57. Found: C, 60.66; H, 4.82; N, 4.27.

Li(1.2)BF$_4$. In an NMR tube flushed with argon, **1** (5 mg, 10.0 mmol) was added to a solution of **2** (6 mg, 10.6 mmol) dissolved in CD_2Cl_2. A first ^{1}H NMR (400 MHz) spectrum of this yellow pale solution was recorded to assume the positions of the different free ligand

signals. $LiBF_4$ (1 mg, 10.6 mmol) was then added to this solution. A very slight orange coloration appeared, and the tube was vigorously stirred until complete dissolution of the salt had occurred. ^1H NMR spectrum and COSY experiments of the mixture were recorded, allowing at least spectroscopic characterization of Li(**1.2**)BF_4 (see below), but further attempts to isolate this labile complex were unsuccessful: it readily decomposes to give free ligands. ^1H NMR (400 MHz, CD_2Cl_2): see text above for **1** signals; for macrocycle **2**,[16] δ (ppm) 8.42 (H_o, d, 4H), 8.30 ($H_{4'}$, d, 2H), 8.09 ($H_{3'}$, d, 2H), 7.77 ($H_{5'}$, d, 2H), 7.23 (H_m, d, 4H), 4.36 (H_α, t, 4H), 3.85 (H_β, t, 4H), 3.76−3.60 (H_γ, H_δ, H_ϵ, m, 12H); for Li(**1.2**)BF_4, δ (ppm) 8.60 (H_4, d, 2H), 8.38 ($H_{4'}$, d, 2H), 8.15 (H_5, s, 2H), 7.84−7.79 ($H_{5'}$, H_3, $H_{3'}$, m, 6H) 7.30 (H_o, d, 4H), 7.16 (H_a, dd, 2H), 7.10 ($H_{c'}$, d, 2H), 6.83 (H_b, dd, 2H), 6.54 ($H_{b'}$, d, 2H), 6.35 (H_c, dd, 2H), 6.05 (H_m, d, 4H), 3.86−3.50 (H_α, H_β, H_γ, H_δ, H_ϵ, m, 20H).

XAS Experiments. A. Sample Preparations. For reference compounds, 2×10^{-3}mol L^{-1} solutions of $Cu(dap)_2BF_4$ and $Cu(dap)_2(BF_4)_2$ in CH_3CN were prepared. For potential dependent XAS measurements, Toray carbon paper TGPH-120 purchased from E-TEK, Inc., was used as the working electrode without any pretreatment, with a surface area measured at 0.27 mg/cm^2. Polymer films were deposited from 2×10^{-3} mol L^{-1} monomer solutions by continuous cycling between −0.2 and 1.4 V by passing 10 mC/cm^2 with a scan rate of 20 mV/s.

B. XAS Measurements. XANES and EXAFS spectra were recorded at the European Synchrotron Research Facility (ESRF, Grenoble, France) on the Collaborative Research Group IF BM 32 beamline equipped with a double-crystal monochromator of Si(111). The harmonics rejection was done with the use of a nickel-coated mirror first and a double platinum-coated mirror second. Energy resolution of the monochromator was $\Delta E/E = 2 \times 10^{-4}$. All the samples have been studied at the Cu K-edge from 8875 to 9650 eV in the fluorescence mode at room temperature. The K_a fluorescence was measured with a Canberra detector containing 27 elements, put perpendicularly to the incident beam, to avoid diffused radiation. The X-ray absorption spectra were converted to an energy scale using copper foil as the internal standard, with the energy of the maximum of the spectrum derivative of the copper foil K-edge defined as 8979 eV. For reference compounds, a Teflon cell windowed with Kapton was used. For experiments under controlled potential, a special cell was designed in our laboratories. The deposition face of the working electrode was laid on the front of the cell as close as possible to the Kapton window. After the filling of the cell with supporting electrolyte, a pseudo reference Ag wire electrode (0.3 mm diameter) was introduced inside the electrolyte compartment sandwiched between the two Toray carbon paper electrodes connected to the PAR 273A via platinum crowns. The position of the samples was approximately at 45° from incident beam to maximize fluorescent detection. All potentials in these experiments are calculated such as $E_{1/2}$ (Cu^I/Cu^{II}) = 0.51 V (i.e., the value observed for this redox system in a classical three-electrode compartment with a 0.01 mol L^{-1} Ag^+/Ag reference electrode). The electrode potential was set to the desired value and acquisition started after stabilization of current to a negligible value.

C. Data Analysis. The analysis was made in harmonic approximation with plane waves[26] using a program developed by D. Aberdam.[27] For a given sample, each scan was first normalized by the height of the absorption jump at the edge, and after comparison of the XAS spectra measured for each scan, the average of two or three scans was calculated to obtain the final spectrum. The extraction of EXAFS oscillations from the final spectrum was accomplished using the procedure described by D. Aberdam.[27] The data were then converted in the k-space and the resultant EXAFS data were k^2 or k^3 weighted (all of the $k^n\chi(k)$ ($n = 1$, 2, 3) data were tested, and the data giving the best shell drawing was then chosen) and Fourier transformed typically from 3 to 13.0 Å^{-1} with an apodization window of Kaiser with plateau. A region of the Fourier transform encompassing the first shell (typically between 0.9 and 2.15 Å) was then backtransformed, weighted by the statistical noise to yield the filtered EXAFS. The noise was estimated in the $k^n\chi(k)$ data by computing the difference between the raw experimental signal and the filtered one. The statistical error is taken as the mean root square value of this difference. McKale[25] functions were first of all used to fit the experimental data to theoretical data for our reference compounds. The amplitude reduction factor (S_0^2) was held constant at 0.8, and the following parameters were allowed to vary during fitting: R_i (distance of the absorber to the scatterers for the shell i), N_i (the number of scatterers at the distance R_i), σ_i^2 (the Debye−Waller factor which contains a thermal agitation component and a standard deviation component of the distance distribution), E_0 (the energy of the edge), and γ and η components of the mean free path l of the ejected photoelectron. After optimization of the parameter values consistent with previously reported crystallographic data,[21,22] phase and amplitude functions were extracted from the model compounds $Cu(dap)_2BF_4$ and $Cu(dap)_2(BF_4)_2$. Phase and amplitude extracted functions of each reference solution were used to model the other; parameters obtained were the same as those obtained with McKale type functions, assuming the validity of the procedure. Consequently, these phase and amplitude extracted functions were used to model the polymer samples. l and ΔE_0 were held fixed at the calibrated values and the parameters R_i, σ_i^2, and N_i were deduced for each shell. Since N_i and σ_i^2 are strongly correlated, N_i was held fixed to chemically reasonable integer values in accordance with XANES qualitative analysis and only R_i and σ_i^2 were optimized.

Acknowledgment. We thank D. Aberdam (CNRS), L. Jacquamet, and M. Billon (CEA Grenoble) for helpful discussions. G. Auzet (CEA Grenoble) is gratefully acknowledged for his help in the design and the building of the sample cells. Y. Soldo and the technical staff of the BM32 beamline at the ESRF are thanked for technical guidance. European Communities are thanked for financial support.

IC990516N

(26) Teo, B. K. In *EXAFS Spectroscopy; Techniques and applications*; Teo, B. K., Joy, D. C., Eds.; Plenum Press: New York, 1981.

(27) (a) Aberdam, D. 1997. The program and its guideline file can be found at the following Internet address: http://www.esrf.fr/computing/expg/subgroups/theory/xafs/aberdam.html. (b) Aberdam, D. *J. Synchrotron Radiat.* **1998**, *5*, 1287.